

Photo-induced sliding transition into a hidden phase in van der Waals materials

Jiajun Li,^{1,2} Philipp Werner,² Michael A. Sentef,³ and Markus Müller¹

¹Laboratory for Theoretical and Computational Physics,
Paul Scherrer Institute, 5232 PSI Villigen, Switzerland

²Department of Physics, University of Fribourg, 1700 Fribourg, Switzerland

³Max Planck Institute for the Structure and Dynamics of Matter,
Center for Free-Electron Laser Science (CFEL), Luruper Chaussee 149, 22761 Hamburg, Germany

(Dated: November 15, 2022)

We propose a generic scenario for metastability and excitation-induced switching in layered materials. Focusing on a minimal bilayer stack, where each layer consists of a honeycomb lattice with A and B sublattices, we map out the energy landscape with respect to the relative sliding of the layers. The sliding affects the interlayer hopping, which induces a splitting between bonding and anti-bonding bands. When this splitting is large, the AA and AB stacking configurations correspond to the global and secondary minima, respectively, and these configurations are separated by a barrier against layer-sliding. While chemical doping only flattens this barrier, strong *photodoping* from bonding to antibonding bands can transiently destabilize the global minimum and induce a sliding motion toward the AB stacked configuration, thereby switching from an equilibrium insulator to a nearly gapless metastable phase. This hopping-driven effect is enhanced by local repulsive interactions, which increase the gap and facilitate the inter-layer sliding.

The engineering of on-demand properties of quantum materials via ultrafast laser excitation is a rapidly growing field [1, 2]. One promising direction is the exploration of nonthermal pathways to control the crystal lattice and thereby the electronic properties of a given material. Layered van der Waals materials are an ideal platform for such explorations. The weak bonding between internally rigid layers opens opportunities to design and manipulate these systems [3, 4]. Since the first fabrication of graphene, the art of stacking atomically thin layers into precisely controlled heterostructures has developed into a routine technology for exploring new material properties that are very sensitive to the nature of the stacking. A prominent example are Moiré superlattices, that can be used as tunable quantum simulators [5–7].

Due to the weak interlayer correlations, the individual rigid layers can slide relative to each other when the energy landscape is modulated, as has recently been observed in WTe₂ [8] and hBN multilayers [9, 10]. Certain stacking configurations result in an electric dipole moment whose coupling to a strong electric field allows for controllable sliding into an otherwise metastable stacking configuration [11–13].

The effect of the stacking arrangement on the electronic structure of the low-temperature phase of 1T-TaS₂ has also been the subject of numerous recent investigations [14–17]. In this correlated material, the stacking pattern of the surface layers can be altered on ultrafast timescales using either laser [18–20] or strong electric-field pulses [21–25]. These nonequilibrium manipulations result in a metallic hidden phase which seems inaccessible under equilibrium conditions [18]. While the strong pulses excite phonons, they also modulate the electronic kinetic energy through photodoping [20, 26], and thus the precise nonthermal pathway toward the hidden stacking

pattern has remained unclear.

Inspired by such experiments, we propose here a concrete and generic scenario in which a substantial photoinduced transfer of electrons to unoccupied antibonding bands induces interlayer sliding toward an initially metastable state in a bilayer material, realizing a solid-state analogon of photo-induced conformation changes in molecules. Our aim is two-fold: We introduce a minimal tight-binding model whose electronic kinetic energy exhibits an asymmetric double-well structure (i.e., metastability) in the continuous space of stacking configurations. We further show that photodoping can destabilize the equilibrium stacking and induce spontaneous sliding into the secondary energy minimum, amounting to light-induced stacking shifts.

Model– We consider materials consisting of rigid layers that can slide relative to each other. We assume that the associated variation of the hopping energy dominates over that of the van der Waals attraction, which is usually weak. We consider two parallel (untwisted) rigid lattices separated by a fixed distance b , and characterize the stacking of the layers by a relative shift vector Δ . We describe the coupled layers by a single-orbital electronic Hamiltonian,

$$H[\Delta] = H_0[\Delta] + U \sum_{i\alpha} (n_{i\alpha\uparrow} - 1/2)(n_{i\alpha\downarrow} - 1/2), \quad (1)$$

where $H_0 = -\sum_{ij\alpha\alpha'\sigma} t_{ij;\alpha\alpha'}(\Delta) c_{i\alpha\sigma}^\dagger c_{j\alpha'\sigma}$ is the kinetic energy, with $c_{i\alpha\sigma}^\dagger$ the creation operator of an electron at site i in the layer $\alpha = 1, 2$, while $\sigma = \uparrow, \downarrow$ labels the spin degree of freedom. U is an onsite Coulomb repulsion, and $n_{i\alpha\sigma} = c_{i\alpha\sigma}^\dagger c_{i\alpha\sigma}$. We assume spin degeneracy and thus omit the spin index for simplicity. The hopping amplitudes $t_{ij;\alpha\alpha'}$ are assumed to decay exponentially over a scale ξ , with different prefactors for intra- and

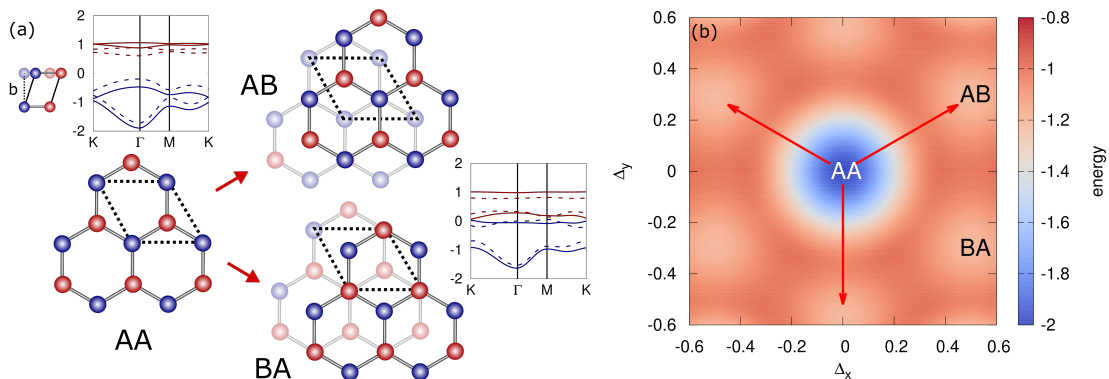


FIG. 1. Kinetic energy $E(\Delta)$ for different stackings of a bilayer of honeycomb lattices. (a) Two likely sliding directions. A unit cell (of side $a = 1$) is delineated by dotted lines. For identical atoms A and B, AB and BA stackings are equivalent. The four bands for AA (left, $\Delta = (0, 0)$) and AB stacking (right, $\Delta = (1/2, \sqrt{3}/6)$) are shown as solid lines. The dashed lines correspond to intermediate shifts $\Delta = (1/5, 0)$ (and $(7/10, \sqrt{3}/6)$), that increase the shortest interlayer atomic distances, as illustrated in the sideview (top left). (b) $E(\Delta)$ as a function of the sliding vector Δ , for parameters $t_1 = 10t_0, \xi = 0.6b$. Six sliding directions lead from the AA-stacked global minimum to AB/BA-stacked local minima.

interlayer hopping, $t_{ij}^{\text{intra}} = t_0 \exp((d_{ij;0} - d_{\min;0})/\xi)$ and $t_{ij}^{\text{inter}} = t_1 \exp((d_{ij;1} - d_{\min;1})/\xi)$ (see supplemental material, SM), with intra- (inter-)layer distances $d_{ij;0}$ ($d_{ij;1}$) and minimal distances $d_{\min;0}$ ($d_{\min;1}$), respectively. t_{ij}^{inter} is maximal ($= t_1$) when the atoms i, j are stacked on top of each other.

Kinetic metastability – As a minimal model to study the hidden phase of a bilayer system, we consider a honeycomb lattice with two atoms (A and B, blue and red in Fig. 1) per unit cell and one electron per atom. We assume A and B to be identical atoms, unlike in interfacial ferroelectrics, although our analysis can be easily generalized. The lattice constant (side of the unit cell in Fig. 1) is $a = 1$, and we assume $b = 0.5a$ [27]. The four bands of the noninteracting model are shown in Fig. 1(a) for AA and AB stacking, exhibiting two or only one pair of strong bonding/antibonding bands, respectively. In equilibrium, the lower two bands are filled. The energy landscape $E(\Delta) = \langle H_e(\Delta) \rangle$ evaluated for $U = 0$ is plotted in Fig. 1(b). Strong bonding bands make AA stacking the global minimum, while AB/BA stacking corresponds to a local minimum. This is generically the case for stackings with fewer pairs of strongly bonding atoms (see SM). Such local minima are often metallic (or tiny-gap semiconductors as in the present model), whereas the AA minimum is insulating, as seen from the inset of Fig. 5(a). This is ensured by a strong interlayer hopping $t_1 \gg t_0$ which separates the bonding and antibonding bands by a substantial hybridization gap. When Δ deviates from $(0, 0)$, the distance between the most closely stacked atoms increases. Accordingly, the interlayer hybridization decreases, the gap shrinks and the total energy increases. At the AB minimum, the high-energy bonding and antibonding bands remain widely separated, while the other two bands approach each other and barely avoid touching in two Dirac points, see the right inset of

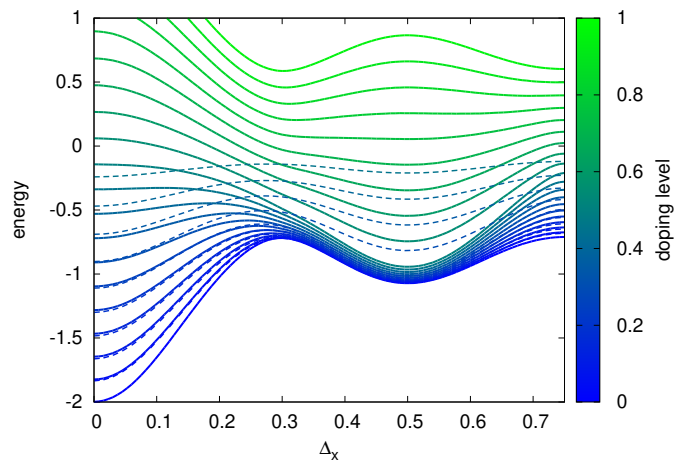


FIG. 2. Photodoping vs. chemical doping. Increasing doping (from blue to green) of either type reduces the energetic difference between the two minima, but only photodoping (solid lines) is capable of destabilizing the global minimum at AA stacking. For photodoping, the doping level f is the fraction of electrons moved from the lower two bands to the upper two bands, and increases by steps of 0.05 between consecutive solid curves. For chemical doping, the hole-doping level $(1 - n)/2$ also increases in steps of 0.05 (dashed lines). A large interlayer hopping $t_1 = 40t_0$ and $\xi = 0.4b$ was chosen to demonstrate the effect clearly.

Fig. 1(a).

Destabilization by photodoping – We now show that photodoping can induce a transition from the global to a local minimum. We restrict ourselves to sliding along the high-symmetry direction $\Delta = \Delta_x(1, \sqrt{3}/3)$ (red arrow in Fig. 1(b)) from AA to AB ($\Delta_x = 1/2$).

Careful photo-excitation protocols in few-layer materials may create an inverted population among the bands near the chemical potential [28], and negative temper-

ature states in extreme cases [29]. Provided that the driving ensures that all bands are occupied close to their bottom, this destabilizes the global minimum (see SM for a general argument in the case of full population inversion) since the energy of the now occupied antibonding bands (red in the insets of Fig. 1) decreases with the band gap as the stacking deviates from AA. The electrons within each band typically thermalize within tens of femtoseconds to an electronic temperature through electron-electron scattering, and cool down within picoseconds to the temperature of the crystal lattice through electron-phonon scattering. In contrast, the inter-band relaxation of a heavily inverted population can take much longer if a large energy gap (exceeding the range of phonon energies) separates the population-inverted bands, and if Auger recombinations are slow as well [30], leaving only very slow radiative recombination, or high-order phonon scattering. This suggests to model the photoinduced electronic distribution after intra-band relaxations by two separate chemical potentials, above and below the central gap.

In the following, we assume that photodoping has transferred a fraction f of the valence electrons to the lowest conduction band states without creating significant entropy, thus assuming a zero-temperature distribution within the bands. This assumption is mainly for convenience, while our conclusions do not depend sensitively on the effective temperature. The resulting sliding energy landscapes are shown in Fig. 2, where we compare off-equilibrium photodoping with equilibrium hole doping (dashed lines). Note that photodoping excites $2f$ electrons per unit cell into the conduction bands, while creating the same density of valence holes. We therefore compare this to a doping of $4f$ holes per unit cell. Although chemical doping flattens the energy landscape, too, only photodoping beyond $f = 0.5$ actually destabilizes the AA stacking. Interestingly, the local minimum at AB stacking remains robust up to very strong photodoping. This is ensured by the remaining bonding bands, while the density of states of the nearly metallic phase near the chemical potential is not very sensitive to sliding. Within a substantial window of photodoping levels the AA minimum is thus destabilized and the system slides spontaneously towards the stable AB minimum.

Sliding to the metastable phase – To analyze the ensuing dynamics of the photo-excited state, we assume the following separation of timescales: As long as a large gap suppresses recombination, the relaxation time of f , τ_{reco} , is much longer than the timescale for sliding τ_{slid} , while both exceed the intraband thermalization timescale τ_{ther} in the nearly metallic phase: $\tau_{\text{reco}} \gg \tau_{\text{slid}} \gg \tau_{\text{ther}}$. With the large gap near AA stacking, the layers will then slide at essentially fixed f . Upon sliding the gap decreases, and we assume that once it drops below a threshold g_* , recombination becomes fast and f decreases rapidly (on the timescale τ_{ther}). The value of g_* depends on the relevant recombination mechanism. If recombination is

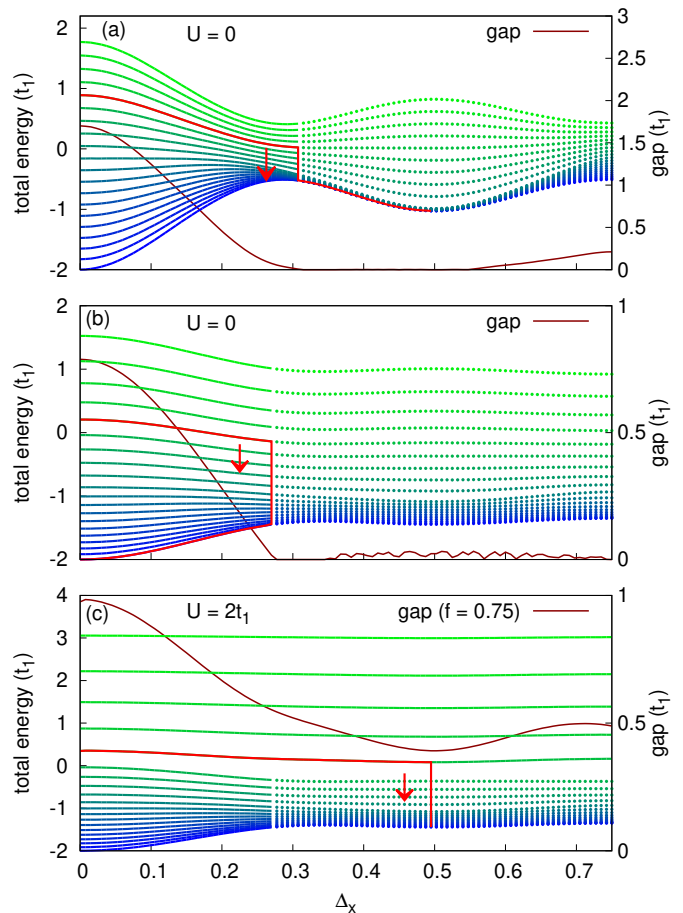


FIG. 3. Non-equilibrium sliding into a minimum for different parameters. Energies are given in units of t_1 . (a) $t_1 = 20t_0$, $\xi = 0.33b$, $U = 0$. (b) $t_1 = 10t_0$ and $\xi = b$, $U = 0$. (c) Same as (b), but with $U = 2t_1$. We use $g_* = 0.2t_0$ as the minimal gap preventing fast recombination. The initial excited fraction f increases by steps of 0.05 from 0 to 0.95 (blue to green). The solid part of a curve corresponds to states with stable inversion ($\text{gap} > g_*$), while photodoping relaxes quickly in the dotted regions. Interactions delay the onset of fast recombination.

induced by phonon scattering, g_* will be of the order of the Debye frequency ω_D .

These considerations suggest the following heuristic rules for the stacking dynamics: (i) The bilayer slides from the destabilized AA stacking toward the non-equilibrium minimum until the gap drops below g_* . (ii) While the gap remains large, f hardly decreases, except if (iii) the system settles into a nonthermal, insulating minimum. In that case f slowly relaxes, while the shift vector adiabatically follows the minimum, potentially until f relaxes to 0. (iv) Once the gap falls below g_* , recombination is enhanced and f rapidly drops to 0. Afterwards, Δ follows the gradient of the equilibrium energy landscape to the nearest local minimum, whereby we assume the electron temperature to remain close to the bath temperature, which we set to $T \approx 0$.

A typical trajectory determined by the above rules is shown in Fig. 3(a). Regions with a large gap are plotted with solid lines while dots indicate a gap $< g_*$. After photodoping a fraction $f = 0.75$ of electrons into the valence band, the layered system slides from the destabilized AA toward the stable AB stacking. As the gap falls below the threshold g_* at some shift Δ^* , the electrons quickly recombine, relaxing to $f = 0$. If Δ^* belongs to the basin of attraction of the AB-stacked metastable minimum the system slides into it. However, depending on parameters, Δ^* might still be too small, so that the layers slide back to AA stacking, as shown in Fig. 3(b).

The hopping parameters for which photo-induced switching to the hidden state succeeds are shown in Fig. 4(a), where we assume an initial photo-doped fraction of $f = 0.75$ to destabilize the global minimum, and a small value of the threshold, $g_* = 0.2t_0$. Without interactions, a relatively short decay length of the hoppings, $\xi/b \lesssim 0.4$, and fairly strong interlayer hoppings t_1/t_0 are required to ensure a pronounced shift-dependent difference between bonding and anti-bonding states and to prevent recombination to set in before the basin of attraction for AB-stacking (at $f = 0$) is reached. The situation changes significantly upon turning on a moderate repulsion $U = 20t_0$. Computing the sliding energy landscape at different f 's using the Hartree-Fock approximation (cf. Fig. 4(b)), we find a substantial interaction gap for large f . As it exceeds g_* , it stabilizes the population inversion to larger Δ and thus allows the system to reach the AB stacked local minimum before fast recombination sets in. This substantially extends the regime of successful switching to the hidden phase (red points). The interaction gap originates from the strong charge imbalance between the two atoms in the unit cell, which become inequivalent under sliding. The interactions also increase the barrier separating the secondary from the global minimum. This arises because a deviation from AB stacking weakens the hopping, which translates into an enhanced interaction gap and thus a higher barrier, as can be seen by comparing the energy landscapes for finite and vanishing U . While the range of deterministically switching non-interacting systems shrinks with increasing threshold g_* (see SM), the stabilization due to interactions is robust and independent of small g_* .

Conclusion and Discussion – Using a minimal electronic model, we have demonstrated that metastable phases exist ubiquitously in the kinetic energy landscape of stacked bilayers with more than one atom per unit cell, and that the stability of stackings can be reversed by a significant non-equilibrium redistribution of electrons between occupied and empty bands using photodoping. In contrast to chemical doping which can only flatten the energy landscape, photodoping is able to destabilize the global minimum upon inverting the band population, inducing spontaneous sliding into a metastable stacking configuration. This provides a pathway for ultrafast op-

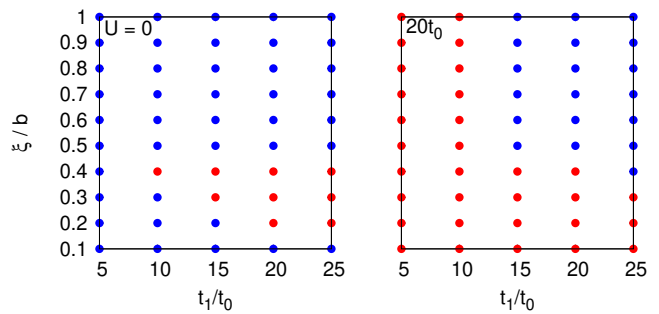


FIG. 4. Switching diagram of photo-induced sliding for a fraction $f = 0.75$ of photodoped electrons and a gap threshold $g_* = 0.2t_0$. Red dots indicate that the hidden phase (AB stacking) is induced deterministically, whereas the system slides back to the AA stacked ground state in the blue region. Left: non-interacting case. Right: a local repulsion $U = 20t_0$ significantly enlarges the successfully switching region.

tically controlled switching to hidden phases of layered systems. Moderate repulsions further enhance the robustness of the switching by creating a nonequilibrium interaction gap that suppresses fast recombination and preserves the electronic population inversion while the layers slide toward their metastable stacking configuration. However, since stronger interactions entail faster Auger recombination, the relevant value of g_* may increase with U , with the danger of fast recombination setting in too early. In such cases, one may have to resort to continuous photo-doping to nevertheless maintain the population inversion during the sliding process.

A uniform sliding of macroscopic layers is unlikely. Indeed, since there are several equivalent sliding directions and secondary minima, different domains may slide in different directions, resulting in a mosaic-like structure [22].

The present study was partially motivated by the hidden phase of $1T$ -TaS₂. Despite the simplicity of our model, some of our findings are qualitatively consistent with experimental observations: For example, it has been shown that lattice defects and doping with Ti help to form the metallic [31] hidden state [32, 33], which can be rationalized by the flattening of the energy surface by chemical doping. The laser driving employed so far, for instance in Ref. 18, may not have been able to create a strongly inverted population, and the resulting weak photodoping has probably had an effect resembling that of chemical doping. Our results, however, predict that an inverted population, created by strong and carefully designed pulses with a chirped frequency that tracks the difference between the two effective chemical potentials [34], can facilitate the formation of the hidden phase, possibly on yet faster time scales than other excitation protocols. As strong inverted band populations can overcome even high energy barriers, our findings also suggest

an alternative non-thermal pathway to induce sliding interfacial ferroelectricity in a wider range of materials.

The present theoretical description could be extended to incorporate *ab initio* input, replacing atomic sites with Wannier orbitals from first-principles calculations. While we expect our heuristic rules to predict the sliding pathway correctly, a quantitative prediction of the switching time would require time-dependent simulations for the combined lattice and electronic dynamics. This could be achieved with Quantum Boltzmann equation methods assisted by dynamical mean-field theory [35, 36] or Ehrenfest dynamics within time-dependent density functional theory [37].

The sliding of layered materials can be seen as a solid-state analogue of photoisomerization, i.e., molecular conformation changes induced by electronic excitations [38]. Those often owe their efficiency to conical intersections of the ground and excited energy surfaces, which funnel the dynamics of the atoms toward a ‘hidden’ conformation [39]. This contrasts with our case where the system slides to a secondary minimum without any intersection, the closing of the band gap being preferentially prevented rather than promoted. However, it would be interesting to explore whether the mechanism we propose for solids, and in particular its boost by interactions, have analogues in molecules or nanophysics.

We acknowledge helpful discussions with D. Baeriswyl, F. Petocchi, M. Eckstein, J. Maklar, and L. Rettig. The project was supported by funding from the European Union’s Horizon 2020 research and innovation programme under the Marie Skłodowska-Curie grant agreement No. 884104, from the ERC Consolidator Grant No. 724103 and from Swiss National Science Foundation Grants Nos. 200021-196966 and 200020.200558. MAS acknowledges financial support through the Deutsche Forschungsgemeinschaft (DFG, German Research Foundation) via the Emmy Noether program (SE 2558/2).

-
- [1] D. Basov, R. Averitt, and D. Hsieh, Towards properties on demand in quantum materials, *Nature materials* **16**, 1077 (2017).
- [2] A. de la Torre, D. M. Kennes, M. Claassen, S. Gerber, J. W. McIver, and M. A. Sentef, Colloquium: Nonthermal pathways to ultrafast control in quantum materials, *Rev. Mod. Phys.* **93**, 041002 (2021).
- [3] A. K. Geim and I. V. Grigorieva, Van der waals heterostructures, *Nature* **499**, 419 (2013).
- [4] K. Novoselov, o. A. Mishchenko, o. A. Carvalho, and A. Castro Neto, 2d materials and van der waals heterostructures, *Science* **353**, aac9439 (2016).
- [5] Y. Cao, V. Fatemi, S. Fang, K. Watanabe, T. Taniguchi, E. Kaxiras, and P. Jarillo-Herrero, Unconventional superconductivity in magic-angle graphene superlattices, *Nature* **556**, 43 (2018).
- [6] Y. Cao, V. Fatemi, A. Demir, S. Fang, S. L. Tomarken, J. Y. Luo, J. D. Sanchez-Yamagishi, K. Watanabe, T. Taniguchi, E. Kaxiras, *et al.*, Correlated insulator behaviour at half-filling in magic-angle graphene superlattices, *Nature* **556**, 80 (2018).
- [7] D. M. Kennes, M. Claassen, L. Xian, A. Georges, A. J. Millis, J. Hone, C. R. Dean, D. Basov, A. N. Pasupathy, and A. Rubio, Moiré heterostructures as a condensed-matter quantum simulator, *Nature Physics* **17**, 155 (2021).
- [8] Z. Fei, W. Zhao, T. A. Palomaki, B. Sun, M. K. Miller, Z. Zhao, J. Yan, X. Xu, and D. H. Cobden, Ferroelectric switching of a two-dimensional metal, *Nature* **560**, 336 (2018).
- [9] K. Yasuda, X. Wang, K. Watanabe, T. Taniguchi, and P. Jarillo-Herrero, Stacking-engineered ferroelectricity in bilayer boron nitride, *Science* **372**, 1458 (2021).
- [10] M. Vizner Stern, Y. Waschitz, W. Cao, I. Nevo, K. Watanabe, T. Taniguchi, E. Sela, M. Urbakh, O. Hod, and M. Ben Shalom, Interfacial ferroelectricity by van der waals sliding, *Science* **372**, 1462 (2021).
- [11] L. Li and M. Wu, Binary compound bilayer and multilayer with vertical polarizations: two-dimensional ferroelectrics, multiferroics, and nanogenerators, *ACS nano* **11**, 6382 (2017).
- [12] M. Wu and J. Li, Sliding ferroelectricity in 2d van der waals materials: Related physics and future opportunities, *Proceedings of the National Academy of Sciences* **118**, e2115703118 (2021).
- [13] P. Tang and G. E. Bauer, The sliding phase transition in ferroelectric van der waals bilayers, *arXiv preprint arXiv:2208.00442* (2022).
- [14] C. W. Nicholson, F. Petocchi, B. Salzmänn, C. Witteveen, M. Rumo, G. Kremer, F. O. von Rohr, P. Werner, and C. Monney, Modified interlayer stacking and insulator to correlated-metal transition driven by uniaxial strain in $1t\text{-tas}_2$, *arXiv preprint arXiv:2204.05598* (2022).
- [15] Z. Wu, K. Bu, W. Zhang, Y. Fei, Y. Zheng, J. Gao, X. Luo, Z. Liu, Y.-P. Sun, and Y. Yin, Effect of stacking order on the electronic state of $1t\text{-tas}_2$, *Phys. Rev. B* **105**, 035109 (2022).
- [16] S.-H. Lee, J. S. Goh, and D. Cho, Origin of the insulating phase and first-order metal-insulator transition in $1t\text{-tas}_2$, *Phys. Rev. Lett.* **122**, 106404 (2019).
- [17] F. Petocchi, C. W. Nicholson, B. Salzmänn, D. Pasquier, O. V. Yazyev, C. Monney, and P. Werner, Mott versus hybridization gap in the low-temperature phase of $1t\text{-tas}_2$, *Phys. Rev. Lett.* **129**, 016402 (2022).
- [18] L. Stojchevska, I. Vaskivskiy, T. Mertelj, P. Kusar, D. Svetin, S. Brazovskii, and D. Mihailovic, Ultrafast switching to a stable hidden quantum state in an electronic crystal, *Science* **344**, 177 (2014).
- [19] Q. Stahl, M. Kusch, F. Heinsch, G. Garbarino, N. Kretzschmar, K. Hanff, K. Rossnagel, J. Geck, and T. Ritschel, Collapse of layer dimerization in the photo-induced hidden state of $1t\text{-tas}_2$, *Nature communications* **11**, 1 (2020).
- [20] J. Maklar, S. Dong, J. Sarkar, Y. Gerasimenko, T. Pincelli, S. Beaulieu, P. Kirchmann, J. Sobota, S.-L. Yang, D. Leuenberger, *et al.*, Coherent light control of a metastable hidden phase, *arXiv preprint arXiv:2206.03788* (2022).
- [21] M. J. Hollander, Y. Liu, W.-J. Lu, L.-J. Li, Y.-P. Sun, J. A. Robinson, and S. Datta, Electrically driven re-

- versible insulator–metal phase transition in 1t-tas₂, *Nano letters* **15**, 1861 (2015).
- [22] L. Ma, C. Ye, Y. Yu, X. F. Lu, X. Niu, S. Kim, D. Feng, D. Tománek, Y.-W. Son, X. H. Chen, *et al.*, A metallic mosaic phase and the origin of mott-insulating state in 1t-tas₂, *Nature communications* **7**, 1 (2016).
- [23] D. Cho, S. Cheon, K.-S. Kim, S.-H. Lee, Y.-H. Cho, S.-W. Cheong, and H. W. Yeom, Nanoscale manipulation of the mott insulating state coupled to charge order in 1t-tas₂, *Nature communications* **7**, 1 (2016).
- [24] I. Vaskivskiy, I. Mihailovic, S. Brazovskii, J. Gospodaric, T. Mertelj, D. Svetin, P. Sutar, and D. Mihailovic, Fast electronic resistance switching involving hidden charge density wave states, *Nature communications* **7**, 1 (2016).
- [25] J. Ravnik, M. Diego, Y. Gerasimenko, Y. Vaskivskiy, I. Vaskivskiy, T. Mertelj, J. Vodeb, and D. Mihailovic, A time-domain phase diagram of metastable states in a charge ordered quantum material, *Nature communications* **12**, 1 (2021).
- [26] M. Ligges, I. Avigo, D. Golež, H. U. R. Strand, Y. Beyazit, K. Hanff, F. Diekmann, L. Stojchevska, M. Kalläne, P. Zhou, K. Rossnagel, M. Eckstein, P. Werner, and U. Bovensiepen, Ultrafast doublon dynamics in photoexcited 1t-tas₂, *Phys. Rev. Lett.* **120**, 166401 (2018).
- [27] A small *b* captures realistic layers with a large super-unit cell.
- [28] J. Li and J. E. Han, Nonequilibrium excitations and transport of dirac electrons in electric-field-driven graphene, *Phys. Rev. B* **97**, 205412 (2018).
- [29] N. Tsuji, T. Oka, P. Werner, and H. Aoki, Dynamical band flipping in fermionic lattice systems: An ac-field-driven change of the interaction from repulsive to attractive, *Phys. Rev. Lett.* **106**, 236401 (2011).
- [30] This may arise either due to a gap exceeding the relevant electronic bandwidths, or more generally due to the weakness of Coulomb-mediated Auger processes that involve relatively large momentum transfers.
- [31] Note that our model contains an even number of electrons per unit cell while for 1T-TaS₂ it is odd. This leads to a metallic (rather than semiconducting) secondary minimum. This difference should, however, not change the sliding scenario qualitatively.
- [32] B. Salzmann, E. Hujala, C. Witteveen, B. Hildebrand, H. Berger, F. O. von Rohr, C. W. Nicholson, and C. Monney, Observation of the metallic mosaic phase in 1t-tas₂ at equilibrium, arXiv preprint arXiv:2209.07945 (2022).
- [33] W. Zhang, J. Gao, L. Cheng, K. Bu, Z. Wu, Y. Fei, Y. Zheng, L. Wang, F. Li, X. Luo, *et al.*, Visualizing the evolution from mott insulator to anderson insulator in ti-doped 1t-tas₂, *npj Quantum Materials* **7**, 1 (2022).
- [34] P. Werner, M. Eckstein, M. Müller, and G. Refael, Light-induced evaporative cooling of holes in the hubbard model, *Nature Communications* **10**, 1 (2019).
- [35] A. Picano, J. Li, and M. Eckstein, Quantum boltzmann equation for strongly correlated electrons, *Phys. Rev. B* **104**, 085108 (2021).
- [36] A. Picano, F. Grandi, and M. Eckstein, Inhomogeneous disordering at a photo-induced charge density wave transition, arXiv preprint arXiv:2112.15323 (2021).
- [37] N. Tancogne-Dejean, M. J. T. Oliveira, X. Andrade, H. Appel, C. H. Borca, G. L. Breton, F. Buchholz, A. Castro, S. Corni, A. A. Correa, U. D. Giovannini, A. Delgado, F. G. Eich, J. Flick, G. Gil, A. Gomez, N. Helbig, H. Hübener, R. Jestädt, J. Jornet-Somoza, A. H. Larsen, I. V. Lebedeva, M. Lüders, M. A. L. Marques, S. T. Ohlmann, S. Pipolo, M. Rampp, C. A. Rozzi, D. A. Strubbe, S. A. Sato, C. Schäfer, I. Theophilou, A. Welden, and A. Rubio, Octopus, a computational framework for exploring light-driven phenomena and quantum dynamics in extended and finite systems, *The Journal of Chemical Physics* **152**, 124119 (2020).
- [38] M. Garavelli, P. Celani, F. Bernardi, M. Robb, and M. Olivucci, The c5h6nh₂⁺ protonated Schiff base: an ab initio minimal model for retinal photoisomerization, *Journal of the American Chemical Society* **119**, 6891 (1997).
- [39] T. Martinez, Seaming is believing, *Nature* **467**, 412–(2010).
- [40] Usually there are additional directional factors taking into account the orientation of chemical bonds. We neglect such factors for simplicity.

Supplementary Materials

Details of the model

The hopping amplitudes are assumed to be simple functions of the atomic distance, $t_{ij;\alpha\alpha'} = t_{\alpha\alpha'} \exp(-(d_{ij;\alpha\alpha'} - d_{\min;\alpha\alpha'})/\xi)$. The shortest distances between atoms from the same layer and from different layers are $d_{\min;11} = d_{\min;22}$ and $d_{\min;12}$, respectively [40]. We take $\mathbf{a}_1, \mathbf{a}_2$ to be two basis vectors of the underlying Bravais lattice. The location of a site i is then $\mathbf{R}_i = n_{i1}\mathbf{a}_1 + n_{i2}\mathbf{a}_2 + \boldsymbol{\delta}_i$, where $\boldsymbol{\delta}_i$ is the relative location of site i in the unit cell.

For intralayer distances, we always have

$$\begin{aligned} d_{ij;\alpha=\alpha'} &= \sqrt{((\mathbf{n}_i - \mathbf{n}_j + \boldsymbol{\delta}_{ij}) \cdot \hat{\mathbf{x}})^2 + ((\mathbf{n}_i - \mathbf{n}_j + \boldsymbol{\delta}_{ij}) \cdot \hat{\mathbf{y}})^2} \\ &= [((n_{i1} - n_{j1} + \delta_{ij,1})a_{1x} + (n_{i2} - n_{j2} + \delta_{ij,2})a_{2x})^2 + ((n_{i1} - n_{j1} + \delta_{ij,1})a_{1y} + (n_{i2} - n_{j2} + \delta_{ij,2})a_{2y})^2]^{1/2}, \end{aligned} \quad (2)$$

where $\boldsymbol{\delta}_{ij} = \boldsymbol{\delta}_i - \boldsymbol{\delta}_j$. Assuming a relative shift $\boldsymbol{\Delta}$ between the layers, the interlayer distance

$$\begin{aligned} d_{ij;12} &= \sqrt{((\mathbf{n}_i - \mathbf{n}_j - \boldsymbol{\Delta} + \boldsymbol{\delta}_{ij}) \cdot \hat{\mathbf{x}})^2 + ((\mathbf{n}_i - \mathbf{n}_j - \boldsymbol{\Delta} + \boldsymbol{\delta}_{ij}) \cdot \hat{\mathbf{y}})^2 + b^2} \\ &= [((n_{i1} - n_{j1} - \Delta_1 + \delta_{ij,1})a_{1x} + (n_{i2} - n_{j2} - \Delta_2 + \delta_{ij,1})a_{2x})^2 + \\ &\quad ((n_{i1} - n_{j1} - \Delta_1 + \delta_{ij,1})a_{1y} + (n_{i2} - n_{j2} - \Delta_2 + \delta_{ij,2})a_{2y})^2 + b^2]^{1/2}. \end{aligned} \quad (3)$$

In general, the interlayer spacing b might itself change slightly with $\boldsymbol{\Delta}$, but we neglect such a dependence for simplicity.

Robustness of the secondary minimum

In the main text we have focused on an undistorted honeycomb lattice. However, the existence of the local minima is robust with respect to distortions of the lattice. In Fig. 5 we show the energy landscape to exhibit a secondary minimum for a wide set of different positions of the B atom within the unit cell. Meanwhile, the sublattice of the A atoms is fixed to remain triangular.

Inverted energy landscape under negative temperatures

Here we show that a negative-temperature distribution always reverses the sign of the slope of the energy landscape and thus destabilizes all minima. In the limit of infinite negative temperature $\beta \rightarrow \infty$ this describes the case of a full band inversion due to extreme photodoping ($f \rightarrow 1$), and thus shows that the latter destabilizes all minima.

We assume $H = H_0$ and $t_{ij;\alpha\bar{\alpha}} = t_{ji;\bar{\alpha}\alpha}$. The derivative of the energy w.r.t $\boldsymbol{\Delta}$ is

$$\partial \langle H_0 \rangle / \partial \boldsymbol{\Delta} = - \sum_{i,j,\alpha,\bar{\alpha},\sigma} (\partial t_{ij;\alpha\bar{\alpha}} / \partial \boldsymbol{\Delta}) \langle c_{i\alpha\sigma}^\dagger c_{j\bar{\alpha}\sigma} \rangle. \quad (4)$$

Using the subscript β to denote the temperature under which the expectation is taken, we note that

$$\langle c_{i\alpha\sigma}^\dagger c_{j\bar{\alpha}\sigma} \rangle_\beta = \text{Tr}(e^{-\beta(H_0 - \mu N)} c_{i\alpha\sigma}^\dagger c_{j\bar{\alpha}\sigma}), \quad (5)$$

where $N = \sum_{i\alpha\sigma} c_{i\alpha\sigma}^\dagger c_{i\alpha\sigma}$.

We consider the system at fixed chemical potential μ . Applying a particle-hole transformation, $P^\dagger c_{i\alpha\sigma}^\dagger P = c_{i\alpha\sigma}$, leads to $P^\dagger H_0 P = -H_0$ and $P^\dagger N P = 2n_{\text{lat}} - N$, where n_{lat} is the number of lattice sites. We then have ,

$$\begin{aligned} \langle c_{i\alpha\sigma}^\dagger c_{j\bar{\alpha}\sigma} \rangle_\beta &= \text{Tr}(P^\dagger e^{-\beta(H_0 - \mu N)} c_{i\alpha\sigma}^\dagger c_{j\bar{\alpha}\sigma} P) \\ &= \text{Tr}(e^{-\beta(-H_0 - 2\mu n_{\text{lat}} + \mu N)} c_{i\alpha\sigma} c_{j\bar{\alpha}\sigma}^\dagger) \\ &= -e^{2\mu\beta n_{\text{lat}}} \text{Tr}(e^{\beta(H_0 - \mu N)} c_{j\bar{\alpha}\sigma}^\dagger c_{i\alpha\sigma}) \\ &= -e^{2\mu\beta n_{\text{lat}}} \langle c_{j\bar{\alpha}\sigma}^\dagger c_{i\alpha\sigma} \rangle_{-\beta}. \end{aligned} \quad (6)$$

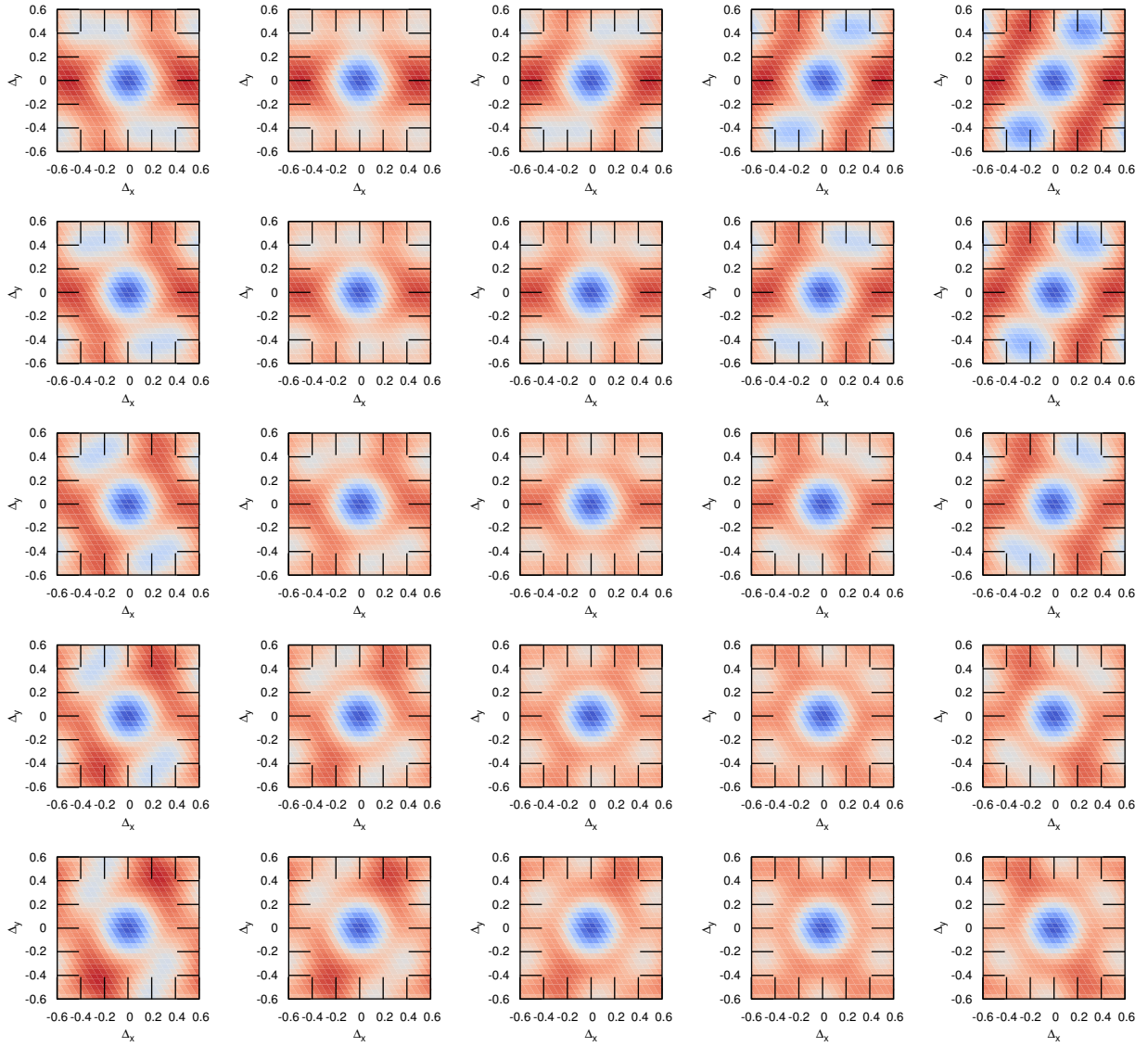


FIG. 5. The energy landscape of a bilayer of distorted hexagonal lattices, where the B atom takes different positions (α_B, β_B) in the unit cell. The columns correspond to $\alpha_B = 0.20, 0.25, \dots, 0.40$, while the rows correspond to $\beta_B = 0.50, 0.55, \dots, 0.70$. The hopping parameters are taken to be $\xi = 0.4b$ and $t_1 = 40t_0$.

From the above equality we obtain

$$\begin{aligned}
 \partial \langle H_0 \rangle / \partial \Delta |_{\beta} &= \sum_{ij\alpha\sigma} \frac{\partial t_{ij;\alpha\bar{\alpha}}}{\partial \Delta} \langle c_{i\alpha\sigma}^{\dagger} c_{j\bar{\alpha}\sigma} \rangle_{\beta} = \frac{1}{2} \sum_{ij\alpha\sigma} \frac{\partial t_{ij;\alpha\bar{\alpha}}}{\partial \Delta} (\langle c_{i\alpha\sigma}^{\dagger} c_{j\bar{\alpha}\sigma} \rangle_{\beta} + \langle c_{j\bar{\alpha}\sigma}^{\dagger} c_{i\alpha\sigma} \rangle_{\beta}) \\
 &= -e^{2\mu\beta n_{1\text{at}}} \frac{1}{2} \sum_{ij\alpha\sigma} \frac{\partial t_{ij;\alpha\bar{\alpha}}}{\partial \Delta} (\langle c_{j\bar{\alpha}\sigma}^{\dagger} c_{i\alpha\sigma} \rangle_{-\beta} + \langle c_{i\alpha\sigma}^{\dagger} c_{j\bar{\alpha}\sigma} \rangle_{-\beta}) \\
 &= -e^{2\mu\beta n_{1\text{at}}} \sum_{ij\alpha\sigma} \frac{\partial t_{ij;\alpha\bar{\alpha}}}{\partial \Delta} \langle c_{i\alpha\sigma}^{\dagger} c_{j\bar{\alpha}\sigma} \rangle_{-\beta}, \\
 &= -e^{2\mu\beta n_{1\text{at}}} \partial \langle H_0 \rangle / \partial \Delta |_{-\beta}.
 \end{aligned} \tag{7}$$

This shows that the slope of the energy landscape in any direction has a sign opposite to that corresponding to positive temperature.

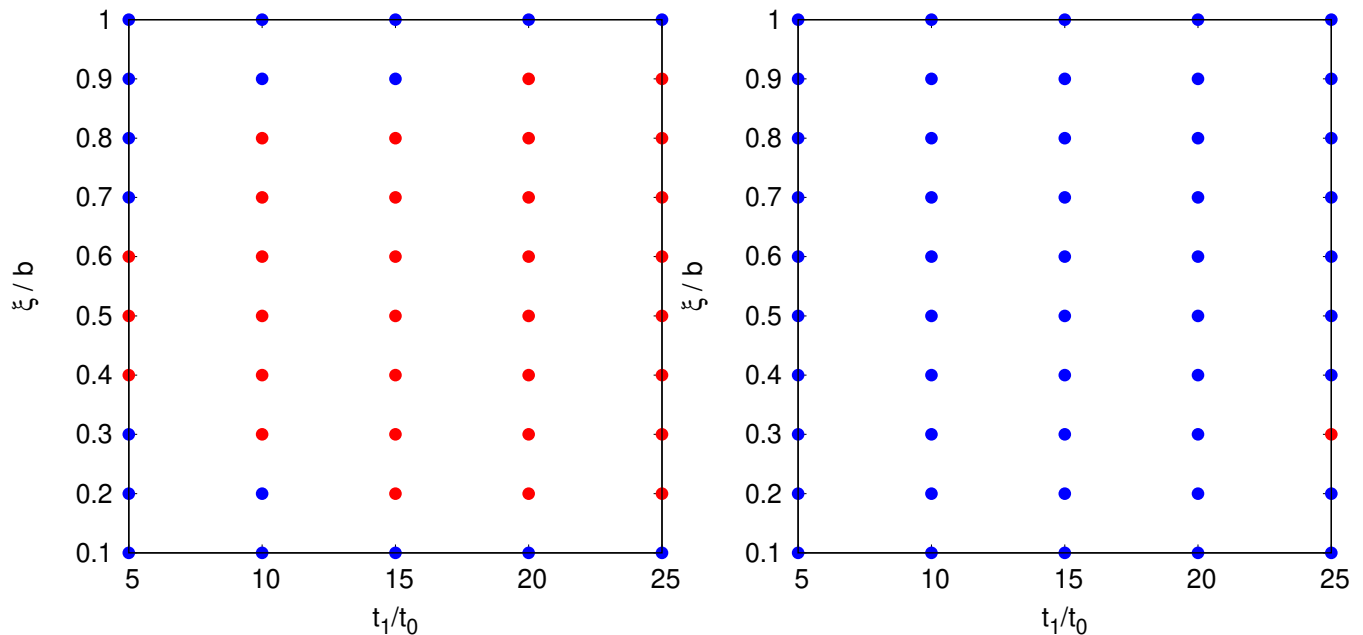


FIG. 6. The switching phase diagram in the non-interacting case ($U = 0$). *Left*: Recombination is assumed to never speed up, i.e., the critical gap is assumed to be $g_* = 0$ (in the numerics we used the value $g_* = 10^{-9}t_0$). *Right*: Recombination is assumed to speed up when the gap falls below the value $g_* = t_0$. We considered the same lattice as in Fig. 4, and the same initial photodoping level of $f = 0.75$

Supplemental data on the dependence of the switching diagram on the gap threshold g_*

Here we study how, in the non-interacting case, the switching diagram depends on the value of the phonon threshold g_* .

On the left of Fig. 6 we show data obtained for the case where we assume that recombination never becomes faster than the sliding motion, corresponding to a threshold gap $g_* = 0$, which is never reached. In this case the switching succeeds in the largest part of parameter space. It fails only if the system does not slide all the way to the minimum that turns into the hidden state upon adiabatic decrease of f , but instead sticks to another minimum which eventually evolves back to the ground state as $f \rightarrow 0$.

We then analyze the case of a gap threshold $g_* = t_0$, which is substantially larger than the value $g_* = 0.2t_0$ considered in Fig. 4. In this case only a tiny pocket of hopping parameter space with very strong bonding tendency still succeeds in switching deterministically.

In this case the deterministic switching of the non-interacting system fails due to the premature de-excitation once the gap reaches the threshold g_* . However, upon de-excitation the system falls close to the maximum of the ground state energy landscape ($f = 0$). Hence, if the de-excitation is not extremely fast compared to sliding time scales, or if fluctuation effects play a role, there may still be a chance that the system slides into the hidden phase, though perhaps just with a finite probability instead of with near certainty. This situation resembles what happens in photoisomerization processes in molecules that are funneled through conical intersections. Also there the evolution is not fully deterministic, but the conformation change has a finite failure rate.

-
- [1] D. Basov, R. Averitt, and D. Hsieh, Towards properties on demand in quantum materials, *Nature materials* **16**, 1077 (2017).
 - [2] A. de la Torre, D. M. Kennes, M. Claassen, S. Gerber, J. W. McIver, and M. A. Sentef, Colloquium: Nonthermal pathways to ultrafast control in quantum materials, *Rev. Mod. Phys.* **93**, 041002 (2021).
 - [3] A. K. Geim and I. V. Grigorieva, Van der waals heterostructures, *Nature* **499**, 419 (2013).
 - [4] K. Novoselov, o. A. Mishchenko, o. A. Carvalho, and A. Castro Neto, 2d materials and van der waals heterostructures, *Science* **353**, aac9439 (2016).

- [5] Y. Cao, V. Fatemi, S. Fang, K. Watanabe, T. Taniguchi, E. Kaxiras, and P. Jarillo-Herrero, Unconventional superconductivity in magic-angle graphene superlattices, *Nature* **556**, 43 (2018).
- [6] Y. Cao, V. Fatemi, A. Demir, S. Fang, S. L. Tomarken, J. Y. Luo, J. D. Sanchez-Yamagishi, K. Watanabe, T. Taniguchi, E. Kaxiras, *et al.*, Correlated insulator behaviour at half-filling in magic-angle graphene superlattices, *Nature* **556**, 80 (2018).
- [7] D. M. Kennes, M. Claassen, L. Xian, A. Georges, A. J. Millis, J. Hone, C. R. Dean, D. Basov, A. N. Pasupathy, and A. Rubio, Moiré heterostructures as a condensed-matter quantum simulator, *Nature Physics* **17**, 155 (2021).
- [8] Z. Fei, W. Zhao, T. A. Palomaki, B. Sun, M. K. Miller, Z. Zhao, J. Yan, X. Xu, and D. H. Cobden, Ferroelectric switching of a two-dimensional metal, *Nature* **560**, 336 (2018).
- [9] K. Yasuda, X. Wang, K. Watanabe, T. Taniguchi, and P. Jarillo-Herrero, Stacking-engineered ferroelectricity in bilayer boron nitride, *Science* **372**, 1458 (2021).
- [10] M. Vizner Stern, Y. Waschitz, W. Cao, I. Nevo, K. Watanabe, T. Taniguchi, E. Sela, M. Urbakh, O. Hod, and M. Ben Shalom, Interfacial ferroelectricity by van der waals sliding, *Science* **372**, 1462 (2021).
- [11] L. Li and M. Wu, Binary compound bilayer and multilayer with vertical polarizations: two-dimensional ferroelectrics, multiferroics, and nanogenerators, *ACS nano* **11**, 6382 (2017).
- [12] M. Wu and J. Li, Sliding ferroelectricity in 2d van der waals materials: Related physics and future opportunities, *Proceedings of the National Academy of Sciences* **118**, e2115703118 (2021).
- [13] P. Tang and G. E. Bauer, The sliding phase transition in ferroelectric van der waals bilayers, *arXiv preprint arXiv:2208.00442* (2022).
- [14] C. W. Nicholson, F. Petocchi, B. Salzmänn, C. Witteveen, M. Rumo, G. Kremer, F. O. von Rohr, P. Werner, and C. Monney, Modified interlayer stacking and insulator to correlated-metal transition driven by uniaxial strain in $1t$ - tas_2 , *arXiv preprint arXiv:2204.05598* (2022).
- [15] Z. Wu, K. Bu, W. Zhang, Y. Fei, Y. Zheng, J. Gao, X. Luo, Z. Liu, Y.-P. Sun, and Y. Yin, Effect of stacking order on the electronic state of $1t$ - tas_2 , *Phys. Rev. B* **105**, 035109 (2022).
- [16] S.-H. Lee, J. S. Goh, and D. Cho, Origin of the insulating phase and first-order metal-insulator transition in $1t$ - tas_2 , *Phys. Rev. Lett.* **122**, 106404 (2019).
- [17] F. Petocchi, C. W. Nicholson, B. Salzmänn, D. Pasquier, O. V. Yazyev, C. Monney, and P. Werner, Mott versus hybridization gap in the low-temperature phase of $1t$ - tas_2 , *Phys. Rev. Lett.* **129**, 016402 (2022).
- [18] L. Stojchevska, I. Vaskivskiy, T. Mertelj, P. Kusar, D. Svetin, S. Brazovskii, and D. Mihailovic, Ultrafast switching to a stable hidden quantum state in an electronic crystal, *Science* **344**, 177 (2014).
- [19] Q. Stahl, M. Kusch, F. Heinsch, G. Garbarino, N. Kretzschmar, K. Hanff, K. Rossnagel, J. Geck, and T. Ritschel, Collapse of layer dimerization in the photo-induced hidden state of $1t$ - tas_2 , *Nature communications* **11**, 1 (2020).
- [20] J. Maklar, S. Dong, J. Sarkar, Y. Gerasimenko, T. Pincelli, S. Beaulieu, P. Kirchmann, J. Sobota, S.-L. Yang, D. Leuenberger, *et al.*, Coherent light control of a metastable hidden phase, *arXiv preprint arXiv:2206.03788* (2022).
- [21] M. J. Hollander, Y. Liu, W.-J. Lu, L.-J. Li, Y.-P. Sun, J. A. Robinson, and S. Datta, Electrically driven reversible insulator-metal phase transition in $1t$ - tas_2 , *Nano letters* **15**, 1861 (2015).
- [22] L. Ma, C. Ye, Y. Yu, X. F. Lu, X. Niu, S. Kim, D. Feng, D. Tománek, Y.-W. Son, X. H. Chen, *et al.*, A metallic mosaic phase and the origin of mott-insulating state in $1t$ - tas_2 , *Nature communications* **7**, 1 (2016).
- [23] D. Cho, S. Cheon, K.-S. Kim, S.-H. Lee, Y.-H. Cho, S.-W. Cheong, and H. W. Yeom, Nanoscale manipulation of the mott insulating state coupled to charge order in $1t$ - tas_2 , *Nature communications* **7**, 1 (2016).
- [24] I. Vaskivskiy, I. Mihailovic, S. Brazovskii, J. Gospodaric, T. Mertelj, D. Svetin, P. Sutar, and D. Mihailovic, Fast electronic resistance switching involving hidden charge density wave states, *Nature communications* **7**, 1 (2016).
- [25] J. Ravnik, M. Diego, Y. Gerasimenko, Y. Vaskivskiy, I. Vaskivskiy, T. Mertelj, J. Vodeb, and D. Mihailovic, A time-domain phase diagram of metastable states in a charge ordered quantum material, *Nature communications* **12**, 1 (2021).
- [26] M. Ligges, I. Avigo, D. Golež, H. U. R. Strand, Y. Beyazit, K. Hanff, F. Diekmann, L. Stojchevska, M. Kalläne, P. Zhou, K. Rossnagel, M. Eckstein, P. Werner, and U. Bovensiepen, Ultrafast doublon dynamics in photoexcited $1t$ - tas_2 , *Phys. Rev. Lett.* **120**, 166401 (2018).
- [27] A small b captures realistic layers with a large super-unit cell.
- [28] J. Li and J. E. Han, Nonequilibrium excitations and transport of dirac electrons in electric-field-driven graphene, *Phys. Rev. B* **97**, 205412 (2018).
- [29] N. Tsuji, T. Oka, P. Werner, and H. Aoki, Dynamical band flipping in fermionic lattice systems: An ac-field-driven change of the interaction from repulsive to attractive, *Phys. Rev. Lett.* **106**, 236401 (2011).
- [30] This may arise either due to a gap exceeding the relevant electronic bandwidths, or more generally due to the weakness of Coulomb-mediated Auger processes that involve relatively large momentum transfers.
- [31] Note that our model contains an even number of electrons per unit cell while for $1T$ - TaS_2 it is odd. This leads to a metallic (rather than semiconducting) secondary minimum. This difference should, however, not change the sliding scenario qualitatively.
- [32] B. Salzmänn, E. Hujala, C. Witteveen, B. Hildebrand, H. Berger, F. O. von Rohr, C. W. Nicholson, and C. Monney, Observation of the metallic mosaic phase in $1t$ - tas_2 at equilibrium, *arXiv preprint arXiv:2209.07945* (2022).
- [33] W. Zhang, J. Gao, L. Cheng, K. Bu, Z. Wu, Y. Fei, Y. Zheng, L. Wang, F. Li, X. Luo, *et al.*, Visualizing the evolution from mott insulator to anderson insulator in ti -doped $1t$ - tas_2 , *npj Quantum Materials* **7**, 1 (2022).
- [34] P. Werner, M. Eckstein, M. Müller, and G. Refael, Light-induced evaporative cooling of holes in the hubbard model, *Nature Communications* **10**, 1 (2019).
- [35] A. Picano, J. Li, and M. Eckstein, Quantum boltzmann equation for strongly correlated electrons, *Phys. Rev. B* **104**,

085108 (2021).

- [36] A. Picano, F. Grandi, and M. Eckstein, Inhomogeneous disordering at a photo-induced charge density wave transition, arXiv preprint arXiv:2112.15323 (2021).
- [37] N. Tancogne-Dejean, M. J. T. Oliveira, X. Andrade, H. Appel, C. H. Borca, G. L. Breton, F. Buchholz, A. Castro, S. Corni, A. A. Correa, U. D. Giovannini, A. Delgado, F. G. Eich, J. Flick, G. Gil, A. Gomez, N. Helbig, H. Hübener, R. Jestädt, J. Jornet-Somoza, A. H. Larsen, I. V. Lebedeva, M. Lüders, M. A. L. Marques, S. T. Ohlmann, S. Pipolo, M. Rampp, C. A. Rozzi, D. A. Strubbe, S. A. Sato, C. Schäfer, I. Theophilou, A. Welden, and A. Rubio, Octopus, a computational framework for exploring light-driven phenomena and quantum dynamics in extended and finite systems, *The Journal of Chemical Physics* **152**, 124119 (2020).
- [38] M. Garavelli, P. Celani, F. Bernardi, M. Robb, and M. Olivucci, The c5h6nh2+ protonated Schiff base: an ab initio minimal model for retinal photoisomerization, *Journal of the American Chemical Society* **119**, 6891 (1997).
- [39] T. Martinez, Seaming is believing, *Nature* **467**, 412– (2010).
- [40] Usually there are additional directional factors taking into account the orientation of chemical bonds. We neglect such factors for simplicity.